Received: 14 June 2019 | Revised: 29 November 2019 | Accepted: 8 January 2020

DOI: 10.4218/etrij.2019-0255

ORIGINAL ARTICLE

ETRI Journal WILEY

An optimization technique for simultaneous reduction of PAPR and out-of-band power in NC-OFDM-based cognitive radio systems

Sravan Kumar Kaliki[1] | **Shiva Prasad Golla**[2] | **Rama Naidu Kurukundu**[2]

[1]Department of Electronics and Communication Engineering, JNT University, Anantapur, Andhra Pradesh, India

[2]Department of Electronics and Communication Engineering, JNTUA College of Engineering, Anantapur, Andhra Pradesh, India

Correspondence
Kaliki Sravan Kumar, Department of Electronics and Communication Engineering, JNT University, Anantapur, Andhra Pradesh, India.
Email: kalikisravanreddy@gmail.com

Noncontiguous orthogonal frequency division multiplexing (NC-OFDM)-based cognitive radio (CR) systems achieve highly efficient spectrum utilization by transmitting unlicensed users' data on subcarriers of licensed users' data when they are free. However, there are two disadvantages to the NC-OFDM system: out-of-band power (OBP) and a high peak-to-average power ratio (PAPR). OBP arises due to side lobes of an NC-OFDM signal in the frequency domain, and it interferes with the spectrum for unlicensed users. A high PAPR occurs due to the inverse fast Fourier transform (IFFT) block used in an NC-OFDM system, and it induces nonlinear effects in power amplifiers. In this study, we propose an algorithm called "Alternative Projections onto Convex and Non-Convex Sets" that reduces the OBP and PAPR simultaneously. The alternate projections are performed onto these sets to form an iteration, and it converges to the specified limits of in-band-power, peak amplitude, and OBP. Furthermore, simulations show that the bit error rate performance is not degraded while reducing OBP and PAPR.

KEYWORDS
IBP, NC-OFDM, OBP, PAPR, peak amplitude

1 | INTRODUCTION

A cognitive radio (CR) system is an intelligent system that detects the subcarriers (white spaces or spectrum holes) that are not used by primary users at a particular instant in time by using a spectrum-sensing scheme. Secondary users utilize these white spaces to transmit their data through the channel. The CR system is a spectrally/bandwidth-efficient technique used in wireless communication systems to achieve higher data rates [1].

Noncontiguous orthogonal frequency division multiplexing (NC-OFDM) is the heart of a CR system. In an OFDM system, the subcarriers are utilized in a contiguous manner, whereas in an NC-OFDM system, utilization of subcarriers is noncontiguous. OFDM and NC-OFDM systems are multicarrier modulation schemes in which a frequency selective channel is converted into a flat fading channel, and consequently, the equalizer used at the receiver is simplified to enable these systems to mitigate inter symbol interference (ISI). However, the NC-OFDM system has two disadvantages: out-of-band power (OBP) and the peak-to-average power ratio (PAPR).

Several methods are proposed in the literature for overcoming the problem of OBP. Active interference cancellation (AIC) [2] and side lobe suppression with orthogonal

projection [3] utilize some subcarriers to reduce OBP but at the cost of a reduction in spectrum efficiency. With extended active interference cancellation [4], the orthogonality of the subcarriers is destroyed, which causes serious interference besides degradation in bit error rate (BER) performance. Pulse shaping (PS) [5] and spectral precoding (SP) [6] have also been proposed in the literature for reducing OBP. However, both have high computational complexity. With regard to reducing PAPR, several techniques have already been proposed in the literature. With clipping, [7] the modulated data are altered, and BER performance is consequently degraded. With the partial transmit sequence method [8], the cost and complexity of systems are increased due to the splitting of inverse fast Fourier transform (IFFT). Active constellation extension [9] and tone reservation (TR) [10] are two other methods for reducing PAPR. These techniques reduce OBP and PAPR individually.

Methods have also been proposed for reducing OBP and PAPR jointly. With the selected mapping algorithm [11], several alternating signals are generated, and the signal with low PAPR and side lobes is selected for transmission. However, this method does not achieve a significant reduction in PAPR and OBP. Furthermore, it requires several subcarriers to reserve side information, resulting in decreased data rates. With signal cancellation (SC) [12], a portion of the outer constellation points on the subcarriers are extended dynamically, and many SC symbols are added to generate the appropriate SC for joint reduction of PAPR and OBP. This method not only degrades the BER performance but also requires more power. One more method proposed is based on using SC and wavelet transform [13] to reduce OBP and PAPR jointly. However, this method requires more power, increases complexity, and also degrades BER performance. Typically, there is a trade-off between PAPR and OBP in any joint reduction technique, that is, reducing one may increase the other. In an earlier study by Liu and Dong, two convex sets are defined to reduce OBP and PAPR jointly [14]. The method uses two algorithms, and in algorithm 1, OBP reduction is superior to that of PAPR, while in algorithm 2, only the PAPR reduction is good. Thus, we propose an algorithm, "Alternative Projection onto Convex and Non-Convex Sets" (APOCNCS), which jointly reduces OBP and PAPR effectively. To this end, we consider two convex sets and add one non-convex set instead of only two convex sets, as in the study by Liu and Dong [14]. Furthermore, computer simulations of BER performance are performed for the model from the previous study and the proposed model.

APOCNCS is such a powerful tool that, with it, we change three parameters (IBP, peak amplitude, and OBP) of the NC-OFDM signal using alternative projections onto three sets. In this method, OBP is the total power present in the null subcarrier band, and IBP is the total power present in the active subcarrier band. This study focuses on further decreasing the PAPR in comparison with the results of the study by Liu and Dong [14]. Therefore, we developed a system model for IBP that increases the total power in the active subcarrier band of the NC-OFDM signal. The first projection is done onto the IBP set, which may increase the peak power of the NC-OFDM signal in the time domain. The second projection is done onto the peak amplitude set, and this reduces the peak power, which may have increased due to the first projection onto the IBP set. Reducing peak amplitude may increase the OBP; consequently, the last projection is done onto the OBP set. This algorithm uses a few subcarriers for adjusting weights, which influences effective data rates. This method does not alter the BER performance of the proposed system.

This paper is organized as follows: The system model is discussed in Section 2. In Section 3, the APOCNCS algorithm is described. Section 4 discusses the analytical expressions of PAPR and BER. The results of the simulations are presented in Section 5, and finally, conclusions are put forward in Section 6.

2 | SYSTEM MODEL

Let us consider a continuous spectrum containing N subcarriers that belong to primary users. Spectrum-sensing detects vacant subcarriers that are not utilized by primary users, and the NC-OFDM system enables us to use these subcarriers for sending the data transmission of secondary users through the communication channel. For NC-OFDM systems, these subcarriers are normally referred to as active subcarriers, and the others are called nulls (ie, null subcarriers). Generally, a discrete-time NC-OFDM signal can be expressed as

$$x[n] = x_n = \frac{1}{\sqrt{N}} \sum_{k=0}^{N-1} X_k e^{j2\pi \frac{kn}{N}}, \quad n = 0, 1, \ldots, N-1, \quad (1)$$

where X_k is the secondary users' data to be transmitted on active subcarriers, $1/NT_s$ is subcarrier spacing, while NT_s and T_s are symbol and sampling periods, respectively.

For accurate calculation of OBP and IBP, the discrete-time NC-OFDM signal is converted to a continuous time NC-OFDM signal using interpolation filter $h_1(t)$. The continuous time NC-OFDM signal can be written as

$$x(t) = h_1(t) \left(\sum_{n=-N_{cp}}^{N-1} x_n \delta(t - nT_s) \right), \quad (2)$$

where N_{cp} is the length of the cyclic prefix (CP). CP is used to reduce ISI due to multipaths. The energy spectrum of $x(t)$ is given as

$$E(f)=\frac{L^2}{N}\left|H_1(f)\sum_{k=0}^{N-1}X_k\mathrm{sinc}_L(f-f_k)e^{-j\pi(f-f_k)T_s(L-2N_{cp}-1)}\right|^2 \quad (3)$$

where $L=N+N_{cp}$, $f_k=\frac{k}{NT_s}$, $H_1(f)$ is the Fourier transform of the interpolation filter $h_1(t)$, and the function sinc_L is defined as

$$\mathrm{sinc}_L(f)=\begin{cases}\frac{\sin(\pi LT_sf)}{L\sin(\pi T_sf)}, & T_sf\notin Z,\\ (-1)^{T_sf(L-1)}, & \text{otherwise},\end{cases} \quad (4)$$

where Z is the set of integers.

The total energy of the NC-OFDM signal can be expressed from the energy spectrum $E(f)$ as

$$E_{\text{Total}}=\int E(f)df. \quad (5)$$

We approximate the energy spectrum of the NC-OFDM signal using N_t evenly spaced frequency samples, and the samples are $\{g_m\}_{m=1}^{N_t}$. We write the total energy of the signal as

$$E_{\text{Total}}\approx\frac{L^2}{N}\Delta_g\sum_{m=1}^{N_t}\left|H_I(g_m)\sum_{k=0}^{N-1}X_k\mathrm{sinc}_L(g_m-f_k)e^{-j\pi(g_m-f_k)T_s(L-2N_{cp}-1)}\right|^2 \quad (6)$$

where Δ_g is the spacing between any two neighboring frequency samples. The total power is linearly proportional to E_{Total} and is given by

$$P_{\text{Total}}=\sum_{m=1}^{N_t}\left|H_I(g_m)\sum_{k=0}^{N-1}X_k\mathrm{sinc}_L(g_m-f_k)\,e^{-j\pi(g_m-f_k)T_s(L-2N_{cp}-1)}\right|^2 \quad (7)$$

$$=\|\mathbf{S}_t\mathbf{X}\|_2^2 \quad (8)$$

Here $\mathbf{S}_t$ is an $N_t\times N$ matrix and

$$\mathbf{S}_t=\begin{pmatrix}S(g_1-f_0) & S(g_1-f_1) & \dots & S(g_1-f_{N-1})\\ S(g_2-f_0) & S(g_2-f_1) & \dots & S(g_2-f_{N-1})\\ \vdots & \vdots & \vdots & \\ S(g_{N_t}-f_0) & S(g_{N_t}-f_1) & \dots & S(g_{N_t}-f_{N-1})\end{pmatrix}$$

where $S(g-f)=H_I(g)\,\mathrm{sinc}_L(g-f)\,e^{-j\pi(g-f)T_s(L-2N_{cp}-1)}$, f_k is the normalized frequency, g_m is the normalized frequency sample within the total measurement range, and $\mathbf{X}$ is $X=[X_0,\ X_1,\ \dots,\ X_{N-1}]^{\mathrm{T}}$.

OBP is the signal power present in the null subcarrier band. Suppose N_{tp} is the number of frequency samples with index K_o consisting of null subcarriers bands, then the total power of these N_{tp} samples is OBP and can be written as

$$P_{\text{OBP}}=\|\mathbf{S}_{tp}\mathbf{X}\|_2^2 \quad (9)$$

where $\mathbf{S}_{tp}$ is an OBP matrix of size $N_{tp}\times N$ and is obtained by eliminating the rows of matrix $\mathbf{S}_t$ that are not indexed in K_o.

Let N_{ts} be the number of samples with index K_I present in the active subcarrier band, then the total number of samples in the NC-OFDM signal is $N_t=N_{tp}+N_{ts}$. The total power of these samples is called as IBP and expressed as

$$P_{\text{IBP}}=\|\mathbf{S}_{ts}\mathbf{X}\|_2^2. \quad (10)$$

$N_{ts}\times N$ is the size of IBP matrix $\mathbf{S}_{ts}$ and is obtained by eliminating the rows of matrix $\mathbf{S}_t$ that are not indexed in K_I.

For example, the subcarriers numbered 0 to 15, 24 to 39, and 48 to 63 are active subcarrier, and the others, numbered 16 to 23 and 40 to 47 are the null subcarriers out of a total of 64 subcarriers (ie, $N=64$). This spectrum is approximated using $N_t=2048$ samples such that each subcarrier spacing has 32 samples. As there are 48 active subcarriers, the total number of samples in the active subcarrier band are $N_{ts}=1536$ (48×32), with index set $K_I=\{1, 2, 3, \dots, 512, 769, \dots, 1280, 1537, \dots, 2048\}$, and the total power of these samples is nothing but IBP. The remaining $N_{tp}=512$ (16×32) samples out of 2048 belong to the null subcarrier band with index set $K_o=\{513, \dots, 768, 1281, \dots, 1536\}$. If we sum up the power in these samples, we obtain the OBP.

In this case, the NC-OFDM signal is oversampled J times to get an accurate peak amplitude and the PAPR of the signal. The oversampled NC-OFDM signal is given by

$$x[n]=x_n=\frac{1}{\sqrt{N}}\sum_{k=0}^{N-1}X_ke^{j2\pi\frac{kn}{JN}},\quad n=0,1,\dots,JN-1. \quad (11)$$

Equation (11) is expressed in discrete-time baseband signal as

$$\mathbf{x}=\mathbf{FX}, \quad (12)$$

where $\mathbf{F}$ is the inverse discrete Fourier transform (IDFT) matrix of size $JN\times N$. We calculate the peak amplitude of the NC-OFDM signal as

$$\Gamma_{\text{Peak}}=\|\mathbf{FX}\|_\infty. \quad (13)$$

By limiting the Γ_{Peak} value, we can limit the peak power of the NC-OFDM signal; hence PAPR can be reduced. The PAPR of the NC-OFDM signal is defined as

$$\text{PAPR}=\frac{\text{Peak power}}{\text{Average power}}=\frac{\max|x_n|^2}{E[|x_n|^2]}. \quad (14)$$

Typically, the oversampling factor J takes an integer, with $J\geq4$, to estimate PAPR accurately.

Similar to the approach used in the study by Liu and Dong [14], some subcarriers are allocated for adjusting weights to reduce OBP and PAPR, and this influences data rates. All the null subcarriers and some active subcarriers are allocated for these weights. The transmitter and receiver block diagrams for the proposed system are presented in Figures 1 and 2, respectively. In the NC-OFDM system, typically, the modulated data vector **d** is directly given to the IFFT block. However, in the proposed system, the model data are given to the IFFT block, as illustrated in Figure 1.

The frequency-domain signal **X** is given as

$$\mathbf{X} = \mathbf{d} + \mathbf{w}, \tag{15}$$

d is complex modulated data vector $\mathbf{d}\varepsilon\mathbf{C}^{N\times 1}$ with non-zero elements at D, such that

$$\mathbf{d}[k] = \begin{cases} d_k, & k \in D, \\ 0, & \text{otherwise}, \end{cases} \tag{16}$$

where D is the index set of the NC-OFDM subcarriers that carry modulated data, and **w** is the complex weight vector $\mathbf{w} \in \mathbf{C}^{N\times 1}$, with non-zero elements at W such that the OBP, IBP, and peak amplitude of the NC-OFDM signal depend on data **X**, which in turn depends on weight vector **w**. Thus, by changing the weight vector **w**, we can reduce the OBP, peak amplitude, and IBP of the NC-OFDM signal.

3 | ALTERNATIVE PROJECTIONS ONTO CONVEX AND NON-CONVEX SETS (APOCNCS) ALGORITHM AND ITS REQUIREMENTS

3.1 | Convex and non-convex sets

We define two convex sets and one non-convex set based on the constraints of the OBP, peak amplitude, and IBP of the NC-OFDM signal, such that

$$A = \{\boldsymbol{X} | \left\| \boldsymbol{S}_{\text{tp}} \boldsymbol{X} \right\|_2^2 \le P_{\text{OBP}}, \left(\boldsymbol{I} - \boldsymbol{I}_{\text{w}}\right) \boldsymbol{X} = \boldsymbol{d}\}, \tag{17}$$

$$B = \{\boldsymbol{X} | \left\| \mathbf{F}\mathbf{X} \right\|_\infty \le \Gamma_{\text{Peak}}, \left(\boldsymbol{I} - \boldsymbol{I}_{\text{w}}\right) \boldsymbol{X} = \boldsymbol{d}\}, \tag{18}$$

$$C = \{\boldsymbol{X} | \left\| \boldsymbol{S}_{\text{ts}} \mathrm{X} \right\|_2^2 \ge P_{\text{IBP}}, \left(\boldsymbol{I} - \boldsymbol{I}_{\text{w}}\right) \boldsymbol{X} = \boldsymbol{d}\}, \tag{19}$$

where P_{OBP} is the OBP limit, Γ_{Peak} is the peak amplitude limit, and P_{IBP} is the IBP limit. **I** is an $N \times N$ identity matrix and $\mathbf{I}_w$ is an $N \times N$ diagonal matrix, defined as

$$\boldsymbol{I}_{\text{w}}[i,i] = \begin{cases} 1, & i \in W, \\ 0, & \text{otherwise}, \end{cases} \tag{20}$$

where $\mathbf{I}_w$ is used to extract non-zero elements of **w** whose indexes are in W.

$$\mathbf{w}[k] = \begin{cases} w_k, & k \in W \\ 0, & \text{otherwise} \end{cases} \tag{21}$$

where W is the index set of the NC-OFDM subcarriers that carry weights.

3.2 | Alternating projections onto convex and non-convex sets

The APOCNCS is such a powerful algorithm that it alters three parameters at a time. The projection operator of vector g onto convex or non-convex set $\mathcal{S}$ is defined as

$$\pi_{\mathcal{S}}(\mathbf{g}) = \arg\min_{\mathbf{f}\in\mathcal{S}} \|\mathbf{g} - \mathbf{f}\|_2 \tag{22}$$

where $\mathcal{S}$ is a convex or non-convex set.

We should take care in assuming the limits of OBP, peak amplitude, and IBP, such that sets A, B, and C should not be empty.

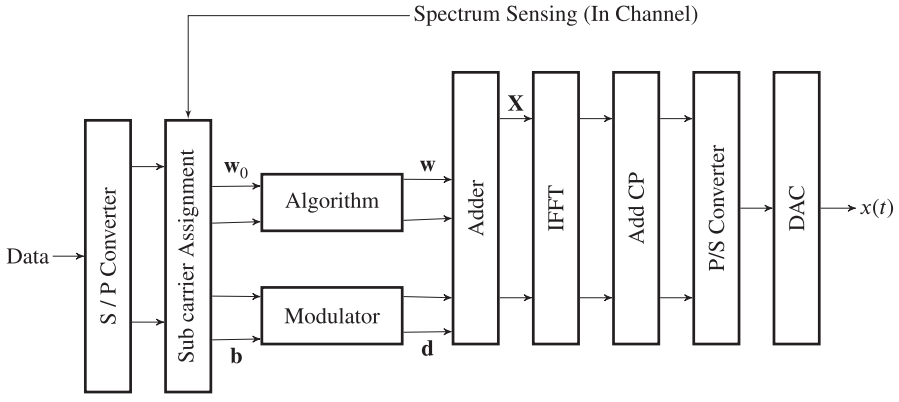

FIGURE 1 Block diagram of the NC-OFDM transmitter

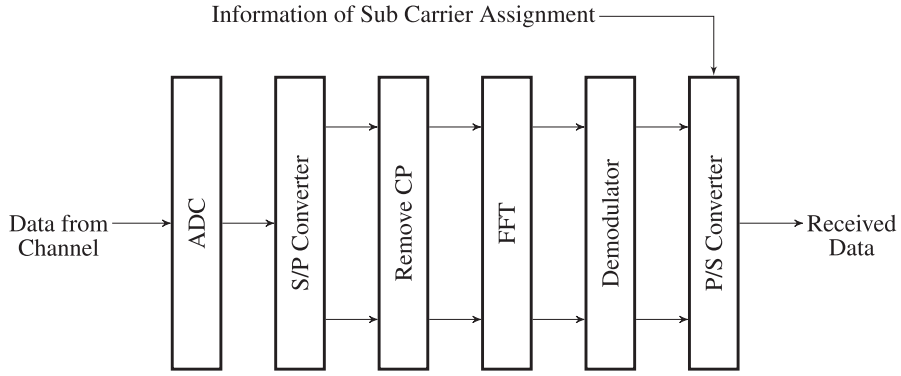

FIGURE 2 Block diagram of the NC-OFDM receiver

If the sets are empty, then the APOCNCS algorithm becomes infeasible, and we do not obtain the solution for the algorithm.

The operator of the projection onto convex set A is

$$\pi_A(\mathbf{X}) = \arg\min_{\mathbf{X}' \in A} \left\| \mathbf{X} - \mathbf{X}' \right\|_2 . \tag{23}$$

The projection onto convex set A from vector $\mathbf{X}$ can be given using mathematical notation as

$$\mathbf{X} = \pi_A(\mathbf{X}) . \tag{24}$$

The solution to (24) can be obtained by solving the following convex optimization problem, which is equal to the projection onto convex set A.

$$\min_{\mathbf{X}'} \left\| \mathbf{X} - \mathbf{X}' \right\|_2 \tag{25}$$

$$\text{subject to: } \left\| \mathbf{S}_{\text{tp}} \mathbf{X}' \right\|_2^2 \le P_{\text{OBP}} \tag{26}$$

$$\left(\mathbf{I} - \mathbf{I}_w \right) \mathbf{X}' = \mathbf{d}. \tag{27}$$

To solve this convex optimization problem, we need convex optimization tools [15].

The operator of the projection onto convex set B is defined as

$$\pi_B(\mathbf{X}) = \arg\min_{\mathbf{X}' \in B} \left\| \mathbf{X} - \mathbf{X}' \right\|_2 . \tag{28}$$

The projection onto convex set B from vector $\mathbf{X}$ can be given as

$$\mathbf{X} = \pi_B(\mathbf{X}) . \tag{29}$$

The solution to (29) can be obtained from the following convex optimization problem.

$$\min_{\mathbf{X}'} \left\| \mathbf{X} - \mathbf{X}' \right\|_2 \tag{30}$$

$$\text{subject to: } \left\| \mathbf{F}\mathbf{X}' \right\|_\infty \le \Gamma_{\text{Peak}} \tag{31}$$

$$\left(\mathbf{I} - \mathbf{I}_{\text{w}} \right) \mathbf{X}' = \mathbf{d}. \tag{32}$$

The operator of the projection onto non-convex set C is given as

$$\pi_C(\mathbf{X}) = \arg\min_{\mathbf{X}' \in C} \left\| \mathbf{X} - \mathbf{X}' \right\|_2 . \tag{33}$$

The projection onto non-convex set C from vector $\mathbf{X}$ can be written as

$$\mathbf{X} = \pi_C(\mathbf{X}) \tag{34}$$

We assume $\tilde{\mathbf{w}}$ and $\tilde{\mathbf{w}}'$ are two $N_w \times 1$ vectors that eliminate zeros from $\mathbf{w}$ and $\mathbf{w}'$, respectively, and $N_w = |W|$, where $|W|$ is the cardinality of set $\mathbf{w}$. For example, if $\mathbf{w} = [\ w_1 \quad 0 \quad 0 \quad w_2\ ]^{\text{T}}$, then $\tilde{\mathbf{w}}$ becomes $\tilde{\mathbf{w}} = [\ w_1 \quad w_2\ ]^{\text{T}}$.

The projection onto set C is equal to the following optimization problem.

$$\min_{\tilde{\mathbf{w}}'} \left\| \tilde{\mathbf{w}} - \tilde{\mathbf{w}}' \right\|_2 \tag{35}$$

$$\text{subject to: } \left\| \mathbf{S}_{\text{ts}} \mathbf{T}_w \tilde{\mathbf{w}}' + \mathbf{S}_{\text{ts}} \mathbf{d} \right\|_2^2 \ge P_{\text{IBP}}, \tag{36}$$

where $\mathbf{T}_w$ is an $N \times N_w$ matrix that recovers $\mathbf{w}$ from $\tilde{\mathbf{w}}$ as $\mathbf{w} = \mathbf{T}_w \tilde{\mathbf{w}}$. For example, if $\mathbf{w} = [\ w_1 \quad 0 \quad 0 \quad w_2\ ]^{\text{T}}$, then

$$\mathbf{T}_w = \begin{pmatrix} 1 & 0 \\ 0 & 0 \\ 0 & 0 \\ 0 & 1 \end{pmatrix}^{\text{T}} .$$

The Karush-Kuhn-Tucker (KKT) condition [14] of problem (36) and (37) is given as

$$2(\tilde{\mathbf{w}}-\tilde{\mathbf{w}}^*)+\lambda\left(2\mathbf{T}_w^{\mathrm{H}}\mathbf{S}_{\mathrm{ts}}^{\mathrm{H}}\left(\mathbf{S}_{\mathrm{ts}}\mathbf{T}_w\tilde{\mathbf{w}}'+\mathbf{S}_{\mathrm{ts}}\mathbf{d}\right)\right)=0 \quad (37)$$

where $\tilde{\mathbf{w}}$ is the optimal solution and λ is the dual variable with respect to the IBP constraints. For a given λ, the $\tilde{\mathbf{w}}^*$ can be obtained using (38), as

$$\tilde{\mathbf{w}}^*=(\mathbf{I}-\lambda\mathbf{T}_w^{\mathrm{H}}\mathbf{S}_{\mathrm{ts}}^{\mathrm{H}}\mathbf{S}_{\mathrm{ts}}\mathbf{T}_w)^{-1}\left(\tilde{\mathbf{w}}+\lambda\mathbf{T}_w^{\mathrm{H}}\mathbf{S}_{\mathrm{ts}}^{\mathrm{H}}\mathbf{S}_{\mathrm{ts}}\mathbf{d}\right). \quad (38)$$

Calculating the vector projected onto a non-convex set C that has the desired $\mathbf{w}$ can be described using the algorithm shown below:

Algorithm:

1. Initialize $\lambda\in(0,1)$.
2. Calculate $\tilde{\mathbf{w}}^*$, based on (38).
3. If $\left\|\mathbf{S}_{\mathrm{ts}}\mathbf{T}_w\tilde{\mathbf{w}}^*+\mathbf{S}_{\mathrm{ts}}\mathbf{d}\right\|_2^2\geq P_{\mathrm{IBP}}$ is not satisfied, repeat from step 2 until above equation converges.
4. $\mathbf{w}=\mathbf{T}_w\tilde{\mathbf{w}}^*$ and $\mathbf{X}=\mathbf{d}+\mathbf{w}$.

In the proposed APOCNCS algorithm, the first projection is done onto non-convex set C, followed by projections onto convex sets B and A to complete an iteration. After performing a few iterations, the proposed algorithm converges to a vector point or limit cycle. The flow chart of the APOCNCS algorithm is presented in Figure 3.

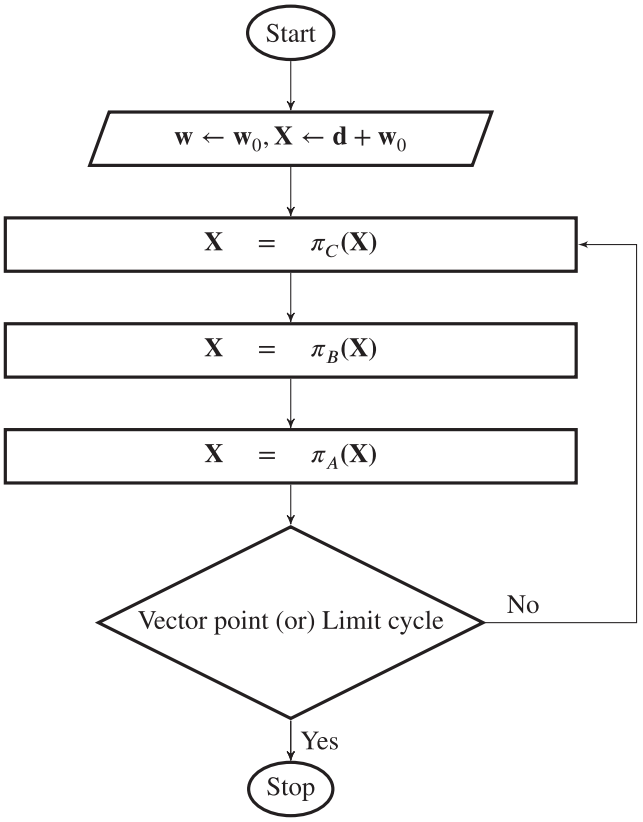

FIGURE 3 Flow chart of APOCNCS algorithm

4 | ANALYTICAL EXPRESSIONS AND COMPUTATIONAL COMPLEXITY

4.1 | Analytical expression of PAPR

Suppose $\mathbf{X}$ is the final data that has been modified by the APOCNCS algorithm based on the limits. Then the analytical expression of PAPR in our system can be given as

$$\mathrm{PAPR}=\frac{\text{Peak power}}{\text{Average power}}=\frac{\|\mathbf{FX}\|_\infty^2}{E\left[|\mathbf{FX}|^2\right]}, \quad (39)$$

where $E[.]$ is the expectation operator.

The complementary cumulative distribution function (CCDF) is widely employed for measuring the PAPR reduction performance, which is defined as the probability that PAPR exceeds a given threshold PAPR_0, That is,

$$\mathrm{CCDF}=Pr\{\mathrm{PAPR}>\mathrm{PAPR}_0\} \quad (40)$$

4.2 | Analytical expression of BER

To evaluate BER, we consider (12) and (15), and the CP is added to (15). This signal is transmitted through the additive white Gaussian noise (AWGN) channel. At the receiver, the NC-OFDM system extracts the modulated data vector corresponding to $\mathbf{d}$, which is demodulated to obtain binary data. We calculate BER by comparing the transmitted and received bits.

The BER expression of the system is

$$P_e=Q\left(\sqrt{\frac{3E_b\log_2 M}{N_o(M-1)}}\right) \quad (41)$$

where M is the number of constellation points in the modulation scheme. For example, M is 4 for the quadrature phase shift keying (QPSK) modulation scheme.

Monte Carlo simulations have been performed to determine BER.

4.3 | Computational complexity

We begin analyzing the computational complexity of convex optimization problem regarding set C as we have made the first projection on to set C. The computational complexity of the projection onto set C is indicated by the number of real multiplications it requires. The convex optimization problem for the projection onto convex set C is defined by an algorithm that uses optimal weight vector $\tilde{\mathbf{w}}^*$, which is calculated based

on (38). In practice, the values of $\mathbf{T}_w^{\mathrm{H}}\mathbf{S}_{\mathrm{ts}}^{\mathrm{H}}\mathbf{S}_{\mathrm{ts}}\mathbf{T}_w$ and $\mathbf{T}_w^{\mathrm{H}}\mathbf{S}_{\mathrm{ts}}^{\mathrm{H}}\mathbf{S}_{\mathrm{ts}}$ can be pre-calculated and stored because matrices $\mathbf{T}_w$ and $\mathbf{S}_{\mathrm{ts}}$ do not change with different transmit data. Then, calculation of $\left(\mathbf{I}-\lambda\mathbf{T}_w^{\mathrm{H}}\mathbf{S}_{\mathrm{ts}}^{\mathrm{H}}\mathbf{S}_{\mathrm{ts}}\mathbf{T}_w\right)$ requires $2N_w^2$ real multiplications. To calculate its inverse, another $2N_w^3$ real multiplications are required, as per the Cholesky decomposition given in [16]. The calculation of $\left(\tilde{w}+\lambda\mathbf{T}_w^{\mathrm{H}}\mathbf{S}_{\mathrm{ts}}^{\mathrm{H}}\mathbf{S}_{\mathrm{ts}}\mathbf{T}_w\mathbf{d}\right)$ requires $2N_w$ real multiplications, given that $\mathbf{T}_w^{\mathrm{H}}\mathbf{S}_{\mathrm{ts}}^{\mathrm{H}}\mathbf{S}_{\mathrm{ts}}\mathbf{d}$ is ready at the start of the algorithm. The calculation of $(\mathbf{I}-\lambda\mathbf{T}_w^{\mathrm{H}}\mathbf{S}_{\mathrm{ts}}^{\mathrm{H}}\mathbf{S}_{\mathrm{ts}}\mathbf{T}_w)^{-1}\left(\tilde{\mathbf{w}}+\lambda\mathbf{T}_w^{\mathrm{H}}\mathbf{S}_{\mathrm{ts}}^{\mathrm{H}}\mathbf{S}_{\mathrm{ts}}\mathbf{T}_w\mathbf{d}\right)$ needs another $4N_w^3$ real multiplications to multiply an $N_w \times N_w$ complex matrix with an $N_w \times 1$ complex vector. Suppose that it takes K iterations for algorithm I to converge, it requires $K\left(2N_w{}^3+6N_w^2+2N_w\right)$ real multiplications for the projection onto non-convex set C. We assume that $(\mathbf{I}-\lambda\mathbf{T}_w^{\mathrm{H}}\mathbf{S}_{\mathrm{ts}}^{\mathrm{H}}\mathbf{S}_{\mathrm{ts}}\mathbf{T}_w)^{-1}$ is pre-calculated and stored with a set of λ's. The number of real multiplications is calculated as $K\left(4N_w^2+2N_w\right)$. The computational complexity of the projection onto non-convex set C is $O\left(N_w^2\right)$.

The projection onto set B and set A requires standard convex optimization tools. It usually has high computational complexity and is hard to analyze [14]. Similar to the computational complexity analysis in [12] and [17], the projection onto the set controlled by the PAPR requirement can be reformulated as a second-order cone program (SOCP). The problem can be solved using the standard interior point method, and the computational complexity is $O(N^3)$ in each iteration. Furthermore, one IDFT operation is required during each iteration, which has a complexity of $O(JN\log JN)$. Therefore, the computational complexity of the projection onto set B is $O(N^3 + JN\log JN)$. The projection onto convex set A defined by the (25), (26), and (27) is reformulated as the algorithm 3 proposed in the study by Liu and Dong [14]. It has computational complexity $O\left(N_{\mathrm{w}}^2\right)$, similar to that of the projection onto non-convex set C. For one iteration, the POCS [14] algorithm has a total computational complexity of $O\left(N_w^2+N^3+JN\log JN\right)$, whereas APOCNCS has a complexity of $O\left(2N_w^2+N^3+JN\log JN\right)$.

From the above discussion, we conclude that the APOCNCS algorithm has greater computational complexity than the previous algorithm (POCS). The computational complexities of the different techniques are presented in Table 1.

TABLE 1 Computational complexity of different techniques

Methods	Complexity
SC (Existing)	$O(N^3 + JN\log JN)$
Sub-SC (Existing)	$O(N^2 + 2JN\log JN)$
POCS (Existing)	$O\left(N_w^2+N^3+JN\log JN\right)$
Proposed - APOCNCS	$O\left(2N_w^2+N^3+JN\log JN\right)$

5 | SIMULATION RESULTS

An NC-OFDM system is considered with 64 subcarriers in simulation. It is assumed that the subcarriers numbered 0 to 15, 24 to 39, and 48 to 63 are active subcarriers, and others numbered 16 to 23, and 40 to 47 are null subcarriers. The QPSK scheme is used to modulate the binary data. We consider $N_{\mathrm{t}} = 2048$, $N_{\mathrm{tp}} = 512$, $N_{\mathrm{ts}} = 1536$, and length of the CP $N_{\mathrm{cp}} = 16$. The chosen subcarriers numbered 0, 5, 10, 15, 24, 29, 34, 39, 48, 53, 58, 63, and the null subcarriers are allocated for adjusting weights to reduce OBP and PAPR. While calculating PAPR, we set the oversampling factor $J = 4$ [14], and the adjusting weights are initialized to zero. Four iterations are considered for the APOCNCS algorithm. BER performance of the system is evaluated through simulations under AWGN channel conditions. The MATLAB software is used for all the simulations, and convex optimization (CVX) tools are added for the execution of convex optimization problems.

Two algorithms (POCS) are proposed in the study by Liu and Dong [14] for reducing the OBP and PAPR simultaneously. However, the proposed algorithms in Liu and Dong's study [14] managed to reduce only one parameter heavily. In the previous algorithm 1, OBP is reduced in the desired manner, but PAPR curves are fallen at initial PAPR curves for the limits (23.7 dB, 0 dB) and (23.7 dB, −4 dB), that is, PAPR reduction performance is not good enough. In the previous algorithm 2, the PAPR reduction is not satisfactory up to a CCDF of 10^{-1}, as the curves follow the initial PAPR curve, and reduction is good after that. However, the limit (23.7 dB, −4 dB) has returned poor results for the reduction of OBP, which are presented in Figures 4 and 5. Normally, there is a trade-off between the PAPR and OBP, such that if we try to reduce PAPR, OBP may increase and vice versa. Thus, if we set the limit of PAPR to less than 23.7 dB, PAPR will decrease, but OBP will increase. When we decrease the OBP from 0 dB to − 4 dB, the PAPR curve shifts right (see Figure 5 for the limits (23.7 dB, 0 dB) and (23.7 dB, −4 dB)).

Thus, we propose an algorithm called APOCNCS that reduces both OBP and PAPR simultaneously. For the limit (43 dB, 23.7 dB, 0 dB), the proposed algorithm reduces OBP from 10.8 dB to 0 dB, and PAPR from 10.85 dB to 8.45 dB, given a CCDF of 10^{-3}. For the same limit, that is, (23.7 dB, 0 dB), the previous algorithm 1 reduces OBP from 10.8 dB to 0 dB, and PAPR from 10.85 dB to 9.63 dB, for a CCDF of 10^{-3}. Thus, the proposed algorithm achieves almost 1.2 dB reduction in PAPR more than the previous algorithm 1 for a CCDF of 10^{-3}. Furthermore, we observe that for the limit (43 dB, 23.7 dB, 0 dB), the reduction of PAPR is better than the two previous (POCS) algorithms up to a CCDF of 10^{-2}. The results of the previous and the proposed algorithms are presented in Tables 2 and 3 for comparison. Even when we decrease OBP to − 10 dB with the proposed algorithm (see

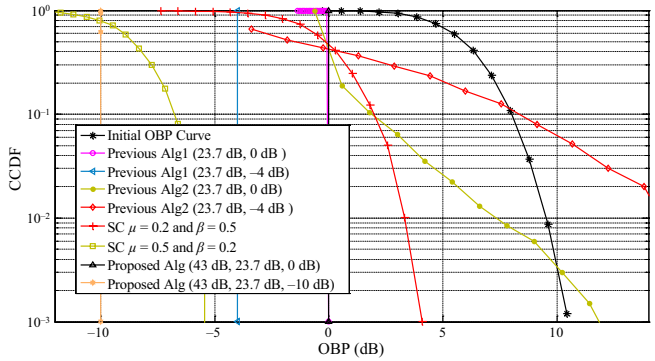

FIGURE 4 OBP(dB) vs CCDF simulation [Colour figure can be viewed at wileyonlinelibrary.com]

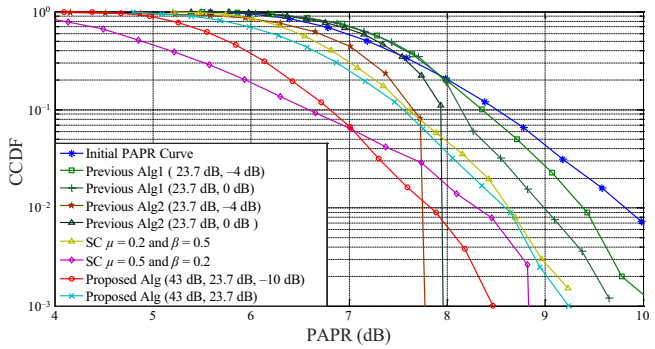

FIGURE 5 PAPR(dB) vs CCDF simulation [Colour figure can be viewed at wileyonlinelibrary.com]

TABLE 2 OBP (dB) vs CCDF results

CCDF	10^{-1}	10^{-2}	10^{-3}
Initial OBP values (dB)	8	9.5	10.8
Previous Alg1 (23.7 dB, 0 dB)	0	0	0
Previous Alg1 (23.7 dB, −4 dB)	−4	−4	−4
Previous Alg2 (23.7 dB, 0 dB)	3.5	7	12.3
Previous Alg2 (23.7 dB, −4 dB)	7.5	16	17.8
SC ($\mu = 0.2, \beta = 0.5$)	2.3	3	4
SC ($\mu = 0.5, \beta = 0.2$)	−7.3	−6	−5.5
Proposed Alg (43 dB, 23.7 dB, 0 dB)	0	0	0
Proposed Alg (43 dB, 23.7 dB, −10 dB)	−10	−10	−10

the result for limit (43 dB, 23.7 dB, −10 dB) in Figure 4), we achieve good reduction in PAPR (see the result for limit (43 dB, 23.7 dB, −10 dB) in Figure 5) that is superior to that of the previous algorithm 1 for the limits (23.7 dB, 0 dB) and (23.7 dB, −4 dB). Thus, the proposed algorithm achieves a more favorable trade-off between OBP and PAPR than the previous algorithm.

The proposed algorithm (APOCNCS) is also compared with the SC method for different μ and β values. The

TABLE 3 PAPR (dB) vs CCDF results

CCDF	10^{-1}	10^{-2}	10^{-3}
Initial PAPR values (dB)	8.6	9.8	10.85
Previous Alg1 (23.7 dB, 0 dB)	8.15	8	9.63
Previous Alg1 (23.7 dB, −4 dB)	8.4	9.2	10.1
Previous Alg2 (23.7 dB, 0 dB)	7.9	7.95	8
Previous Alg2 (23.7 dB, −4 dB)	7.6	7.75	7.79
SC ($\mu = 0.2, \beta = 0.5$)	7.6	8.7	9.3
SC ($\mu = 0.5, \beta = 0.2$)	6.6	7.9	8.85
Proposed Alg (43 dB, 23.7 dB, 0 dB)	6.8	7.86	8.45
Proposed Alg (43 dB, 23.7 dB, −10 dB)	7.5	8.6	9.15

PAPR reduction of SC method improves when the power of the SC method increases, that is, when μ increases and the OBP reduces as β decreases. Thus, we have taken a high μ value (ie, $\mu = 0.5$) and low β value (ie, $\beta = 0.2$), for which both PAPR and OBP reduction performance would be good. It is observed that the reduction in performance of the SC method is comparable in PAPR and is good in OBP when compared with that of APOCNCS for the limit (43 dB, 23.7 dB, 0 dB). However, BER performance is degraded: as reduction performance of the SC method increases, the BER performance is degraded. For lower reduction performance of the SC method, that is, for $\mu = 0.2$ and $\beta = 0.5$, the degradation of BER performance is less but worsens as PAPR and OBP reduction performance increases.

The proposed algorithm does not alter the modulated data. Hence, the BER curve follows the theoretical curve of the NC-OFDM system. The corresponding simulation results are presented in Figure 6. The power spectrum of the NC-OFDM signal for the SC, and the previous and proposed algorithms are presented in Figure 7.

6 | CONCLUSIONS

In this study, we propose an algorithm that jointly reduces the OBP and PAPR effectively, instead of the two POCS algorithms proposed in the literature. From the simulation results, we observe that there is a reduction of 10.8 dB in OBP and 2.2 dB in PAPR at a CCDF of 10^{-3} in the proposed algorithm for the limits (43 dB, 23.7 dB, 0 dB) compared to initial OBP and PAPR curves. Thus, good reduction performance is achieved in both OBP and PAPR. We obtained a favorable trade-off between OBP and PAPR reduction. The proposed algorithm does not alter the modulated data. Hence the BER curve follows the theoretical curve of the NC-OFDM system. As we include a non-convex set in the APOCNCS algorithm,

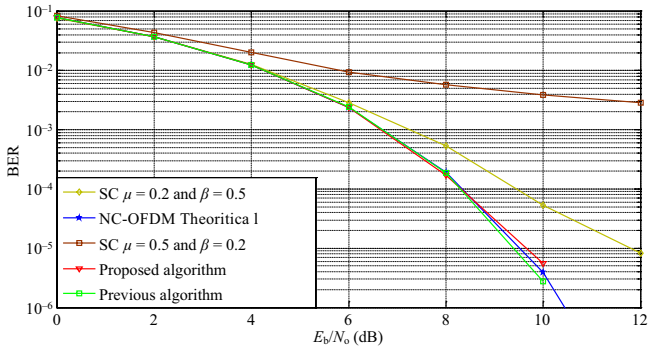

FIGURE 6 BER performance of NC-OFDM system [Colour figure can be viewed at wileyonlinelibrary.com]

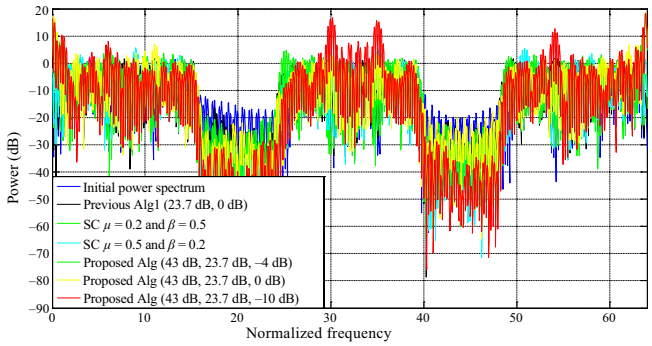

FIGURE 7 Power spectrum of NC-OFDM signal for different algorithms [Colour figure can be viewed at wileyonlinelibrary.com]

the complexity of the algorithm is increased compared to that of the previous algorithm. If there is an intersection among the convex sets, the algorithm converges exactly to the limits of IBP, peak amplitude, and OBP. Here, we altered the three parameters of the NC-OFDM signal using the APOCNCS algorithm to reduce PAPR and OBP simultaneously.

ORCID

Sravan Kumar Kaliki https://orcid.org/0000-0003-1322-7442

REFERENCES

1. B. Wang and K. J. R. Liu, *Advances in cognitive radio networks: a survey*, IEEE J. Selected Topics Signal Process. **5** (2011), no. 1, 5–23.
2. H. Yamaguchi, *Active interference cancellation technique for MB-OFDM cognitive radio*, in Proc 34th Eur. Microw. Conf. (Amsterdam, The Netherlands), Oct. 2004, pp. 1105–1108.
3. J. Zhang et al., *Sidelobe suppression with orthogonal projection for multicarrier systems*, IEEE Trans. Commun. **60** (2012), no. 2, 589–599.
4. D. Qu, Z. Wang, and T. Jiang, *Extended active interference cancellation for sidelobe suppression in cognitive radio OFDM systems with cyclic prefix*, IEEE Trans. Veh. Technol. **59** (2010), no. 4, 1689–1695.
5. R. Xu, H. Wang, and M. Chen, *On the out-of-band radiation of DFT based OFDM using pulse shaping*, in Proc. Int. Conf. Wireless Commun. Signal Process. (Nanjing, China), Nov. 2009, pp. 1–5.
6. W. C. Chen and C.-D. Chung, *Spectral precoding for cyclic-prefixed OFDMA with interleaved subcarrier allocation*, IEEE Trans. Commun. **61** (2013), no. 11, 4616–4629.
7. I. Gutman, I. Iofedov, and D. Wulich, *Iterative decoding of iterative clipped and filtered OFDM signal*, IEEE Trans. Commun. **61** (2013), no. 11, 4284–4293.
8. L. Li and D. Qu, *Joint decoding of LDPC code and phase factors for OFDM systems with PTS PAPR reduction*, Trans. Veh. Technol. **62** (2013), no. 1, 444–449.
9. B. Krongold and D. Jones, *Par reduction in OFDM via active constellation extension*, IEEE Trans. Broadcast. **49** (2003), no. 3, 258–268.
10. H. Li, T. Jiang, and Y. Zhou, *An improved tone reservation scheme with fast convergence for PAPR reduction in OFDM systems*, IEEE Trans. Broadcast. **57** (2011), no. 4, 902–906.
11. A. Ghassemi et al., *Joint sidelobe and peak power reduction in OFDM-based cognitive radio*, in Proc. IEEE 72nd Veh. Technol. Conf. Fall (Ottawa, Canada), Sept. 2010, pp. 1–5.
12. C. Ni, T. Jiang, and W. Peng, *Joint PAPR reduction and sidelobe suppression using signal cancellation in NC-OFDM-based cognitive radio systems*, IEEE Trans. Veh. Technol. **64** (2015), no. 3, 964–972.
13. A. I. Zak et al., *Joint PAPR reduction and sidelobe suppression in NC-OFDM based cognitive radio using wavelet packet and SC techniques*, Phys. Commun. **35** (2019), 1–9.
14. Y. Liu and L. Dong, *Iterative reduction of out-of-band power and peak-to-average power ratio for non-contiguous OFDM, systems based on POCS*, IEICE Trans. Commun. **E100–B** (2017), no. 8, 1489–1497.
15. S. Boyd and L. Vandenberghe, Convex Optimization, Cambridge University Press, 2004.
16. A. Krishnamoorthy and D. Menon, *Matrix inversion using Cholesky decomposition*, in Proc. Signal Process.: Algorithms, Architectures, Arrangements, Applicat. (Poznan, Poland), Sept. 2013, pp. 70–72.
17. H. H. Bauschkey and J. M. Borweiny, *On projection algorithms for solving convex feasibility problems*, SIAM REV. **38** (1996), 367–426.

AUTHOR BIOGRAPHIES

Sravan Kumar Kaliki received his BE in Electronics and Communication Engineering from Anna University, Chennai in 2005, and MTech from SRM University, Chennai, in 2007. He is currently pursuing a Ph.D. at the Department of ECE, Jawaharlal Nehru Technological University Anantapur, Ananthapuramu, India. His research interests are Wireless Communications and Signal Processing.

Shiva Prasad Golla received his BTech degree in Electronics and Communication Engineering from Madanapalle Institute of Technology and Science, Andhra Pradesh in 2013, and his MTech degree in Digital Electronics and Communication systems from JNTUA CEA, Ananthapuramu. Presently working as a Project Scientist-1 at the National Institute of Ocean Technology, Chennai, his main research interests are Communications and Signal Processing.

Rama Naidu Kurukundu received BTech degree (Electronics and Communication Engineering) from Jawaharlal Nehru Technological University, Ananthapuramu in 1983, the MTech (Microwave Engineering) from Indian Institute of Technology, Banaras Hindu University, in 1990, and a Ph.D. from Indian Institute of Technology, Kharagpur, in 2009. At present, he works as a Professor in the Department of ECE at JNTUA College of Engineering Anantapur, Ananthapuramu, India. His research interests include Wireless Communications, Signal Processing, Antennas, and Microwave Engineering.